

Plasmon dromions in a metamaterial via plasmon-induced transparency

Zhengyang Bai¹ and Guoxiang Huang^{1,2,*}¹State Key Laboratory of Precision Spectroscopy and Department of Physics, East China Normal University, Shanghai 200062, China²NYU-ECNU Joint Institute of Physics at NYU-Shanghai, Shanghai 200062, China

(Received 24 November 2015; published 13 January 2016)

We propose a scheme to realize a giant Kerr nonlinearity and create stable high-dimensional nonlinear plasmon polaritons via plasmon-induced transparency (PIT) in a metamaterial, which is constructed by an array of unit cell consisting of a cut-wire and a pair of varactor-loaded split-ring resonators. We show that, due to the PIT effect and the nonlinearity contributed by the varactor, the system may possess very large second-order and third-order nonlinear susceptibilities. We further show that the system supports a resonant interaction between longwave and shortwave and hence effective third-order nonlinear susceptibility can be further enhanced one order of magnitude. Based on these peculiar properties, we derive Davey-Stewartson equations governing the evolution of longwave and shortwave envelope, and demonstrate that it possible to generate plasmon dromions [i.e., (2+1)-dimensional plasmon solitons with coupled longwave and shortwave components] with very low generation power. Our study raises the possibility for obtaining new, giant Kerr effect and stable high-dimensional nonlinear plasmon polaritons at very low radiation intensity by using nonlinear PIT metamaterials.

DOI: [10.1103/PhysRevA.93.013818](https://doi.org/10.1103/PhysRevA.93.013818)

I. INTRODUCTION

In recent years, much attention has been paid to the investigation on the classical analog of atomic electromagnetically induced transparency (EIT) [1] in various physical systems, such as coupled resonators [2,3], electric circuits [2–4], optomechanical devices [5,6], whispering-gallery-mode microresonators [7], various metamaterials (see, e.g., Refs. [8–21]), etc. In particular, the plasmonic analog of atomic EIT in metamaterials, called plasmon-induced transparency (PIT) [8–10], is a very fruitful platform for the study of EIT-like propagation of plasmonic polaritons in solid-state systems [11,13,15–17].

PIT is a typical destructive interference effect resulting from the strong coupling between the wide-band bright mode and the narrow-band dark mode in meta-atoms of metamaterials. The most distinctive characteristics of PIT is the appearance of transparency window within broadband absorption spectrum, along with extraordinarily steep dispersion and dramatic reduction in the group velocity of plasmonic polaritons. PIT metamaterials can not only work in different regions of radiation frequency (including microwave [9], terahertz [10,13,16], infrared, and visible radiations [8,11,15]), but also can be used to design chip-scale plasmonic devices, in which the radiation damping can be largely suppressed through the destructive interference effect between bright and dark modes. Owing to abundant physical capabilities, important applications of PIT have been proposed, such as low-loss metamaterials [8,10], highly sensitive sensors [12,13,17], optical buffers [14,16], ultrafast optical switches [16], storage and retrieval of electromagnetic pulses [18], and so on.

However, most studies on the plasmon polaritons in PIT metamaterials reported up to now are focused on linear propagation regime. Because of the highly resonant (and hence dispersive) character inherent in PIT metamaterials, linear plasmon polaritons inevitably undergo a significant distortion

during propagation. Furthermore, due to the diffraction effect, which can not be neglected for the cases of small transverse size or long propagation distance, a large deformation of linear plasmon polaritons is unavoidable. Thus it is necessary to seek the possibility to obtain a robust propagation of plasmon polaritons in PIT metamaterials. One way to solve this problem is to make PIT systems work in a nonlinear propagation regime.

In this article, by extending the recent work [19] for (1+1)-dimensional [(1+1)D] nonlinear plasmon polaritons, we propose a scheme to realize a giant Kerr nonlinearity and generate stable (2+1)D nonlinear plasmon polaritons via PIT in a metamaterial, which is constructed by an array of unit cell consisting of a cut-wire (CW) and a pair of varactor-loaded split-ring resonator (SRR). We show that, due to the PIT effect and the nonlinearity contributed by the varactor, the system may possess very large second-order and third-order nonlinear susceptibilities ($\chi^{(2)} \approx 10^{-3} \text{ mV}^{-1}$; $\chi^{(3)} \approx 10^{-6} \text{ m}^2\text{V}^{-2}$). We further show that the system supports a resonant interaction between longwave and shortwave, which happens when $V_p \approx V_g$ [where V_p (V_g) is the phase (group) velocity of the longwave (shortwave)] and can occur in our system in a broad parameter region. Based on such longwave-shortwave interaction, the effective third-order nonlinear susceptibility can be further enhanced one order of magnitude (up to $10^{-5} \text{ m}^2\text{V}^{-2}$). Such a mechanism of enhancing third-order nonlinear susceptibility by using longwave-shortwave resonance was proposed by Newell and Moloney more than twenty years ago [22], but to the best of our knowledge no realistic physical system was found up to date. Based on these peculiar properties, we derive Davey-Stewartson (DS) equations governing the evolution of longwave and shortwave envelope, and demonstrate that it is possible to create plasmon dromions [i.e. (2+1)D plasmon solitons with coupled longwave and shortwave components] with very low generation power.

We notice that some nonlinear effects in PIT systems were considered in Ref. [20,21], in which a nonlinearity was obtained by inserting nonlinear elements (e.g., varactors) into SRR slits. However, our work is different from Refs. [20,21]

*gxhuang@phy.ecnu.edu.cn

where only a single unit cell (meta-atom), i.e., not an effective medium, was adopted and no Kerr effect and plasmon solitons were discussed. Furthermore, our work is also different from that in Ref. [19] where only a (1+1)D problem was considered and no longwave-shortwave resonance was explored; besides, in Ref. [19] no plasmon dromions was predicted and the plasmon soliton obtained is unstable when the diffraction length is comparable with the dispersion length and nonlinearity length. Our study presented here raises the possibility for obtaining a giant Kerr effect and stable high-dimensional nonlinear plasmon polaritons at rather low radiation intensity by the use of nonlinear PIT metamaterials.

The remainder of the article is organized as follows. Section II describes our theoretical model. Section III discusses the linear dispersion relation of the system and derives the DS equations describing the nonlinear propagation of (2+1)D plasmon polaritons; the giant Kerr nonlinearity through PIT and the longwave-shortwave resonance is also discussed. Section IV gives the plasmon dromion solutions and discusses their stability. The last section summarizes the main results obtained in the present work.

II. MODEL

The metamaterial structure considered here is an array of PIT unit cells [16] consisting of a CW and two SRRs with a nonlinear varactor inserted into the slits of the SRRs [see Fig. 1(a) and Fig. 1(b)]. We assume that an incident gigahertz radiation is collimated on the metamaterial array with the electric field parallel to the CW, as illustrated in Fig. 1(c) [16,19]. Orange solid lines in Fig. 1(d) show, respectively, the numerical results of the normalized absorption spectrum as a function of the incident-wave frequency for the sole-CW (i.e., no SRR in the unit cell), for the unit cell with $d = 0.24$ mm (d is the separation between the CW and the SRR pair), and for the unit cell with $d = 0.03$ mm, which are obtained by using the commercial finite difference time domain software package (CST Microwave Studio). We observe that for the sole CW (no PIT in this case), the gigahertz radiation suffers a large, broadband absorption, whereas for the unit cell with SRRs (PIT is present) a transparency window opens in the absorption spectrum and it becomes wider and deeper as d is reduced.

The occurrence of the transparency window in the broadband absorption spectrum can be explained simply as follows. For a normal incident of the radiation, the CW in the unit cell functions as a dipole antenna and thus can serve as a bright mode. The two SRRs in the unit cell function as dark modes, which may be symmetric or antisymmetric. The antisymmetric mode has counterpropagating currents on the two SRRs; therefore, there is no direct electrical dipole coupling with the radiation, and it can be considered as a dark mode of a long dephasing time. The resonance frequency of this dark mode is designed to coincide with that of the bright mode. Hence, the CW and the SRRs serve, respectively, as the bright and dark modes, and their destruction interference leads to a dip at the center of the absorption spectrum (i.e., PIT) [8,16].

The dynamics of the bright and dark modes in the unit cell at the position $\mathbf{r} = (x, y, z)$ can be described by the Lorentz

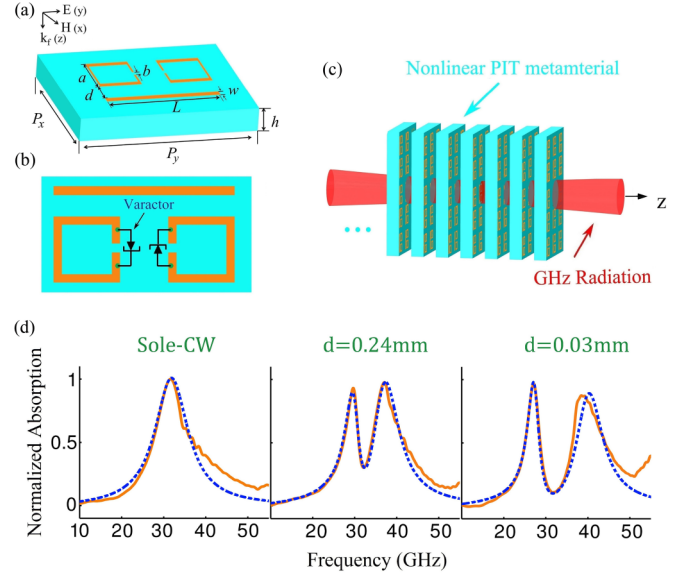


FIG. 1. (a) PIT unit cell consisting of a CW and a pair of SRR. The unit-cell parameters are $L = 1.7$, $w = 0.1$, $a = 0.58$, $b = 0.1$, $P_x = 1.6$, $P_y = 2.4$ (in unit mm). 10- μ m-thick aluminium that forms the CW and the SRR-pair pattern is etched on a Si-on-sapphire wafer comprised of 100- μ m-thick undoped Si film and 2.1-mm-thick sapphire substrate (i.e., $h = 2.21$ mm). (b) SRR pair with a hyperabrupt tuning varactor mounted onto their slits. (c) Suggested experimental arrangement for measuring plasmon dromions. To form plasmon dromions, many (>20) layers in the array of PIT unit cells are assumed. (d) Numerical (orange solid lines) and analytical (blue dashed lines) results of the normalized absorption spectrum as a function of the incident-wave frequency for sole-CW, $d = 0.24$, and $d = 0.03$ (in unit mm), respectively. Analytical result is obtained from solving the model Eqs. (1) and (2) in linear regime.

equations for two coupled oscillators [8,16]

$$\ddot{q}_1 + \gamma_1 \dot{q}_1 + \omega_0^2 q_1 - \kappa^2 q_2 = g E(\mathbf{r}, t), \quad (1a)$$

$$\ddot{q}_2 + \gamma_2 \dot{q}_2 + (\omega_0 + \Delta)^2 q_2 - \kappa^2 q_1 + \alpha q_2^2 + \beta q_2^3 = 0, \quad (1b)$$

where q_1 and q_2 are respectively amplitudes of the bright and dark modes (the dot over q_j denotes time derivative), with γ_1 and γ_2 respectively their damping rates; $\omega_0 = 2\pi \times 32$ GHz and $\omega_0 + \Delta$ are respectively linear natural frequencies of the bright and dark modes ($\gamma_2 \ll \gamma_1 \ll \omega_0$); parameter κ denotes the coupling strength between the CW and SRR pair; g is the parameter indicating the coupling strength of the bright mode with the incident radiation E . The last two terms on the left-hand side of Eq. (1b) are provided by the hyperabrupt tuning varactors mounted onto gaps of the SRRs [23–25]. Thus the metamaterial structure suggested here is a coupled anharmonic oscillator system driven by the incident radiation E . The coefficients α and β characterize the quadratic and cubic nonlinearities of the system, which have important implication for the occurrence of longwave-shortwave resonance, giant effective Kerr effect, and plasmonic dromions discussed in the following. Note that when writing Eq. (1) we have taken a coordinate system in which the electric (magnetic) field E (H) is along y (x) direction and wave vector k_f is along z direction.

The equation of motion for the electric field E is governed by the Maxwell equation

$$\nabla^2 E - \frac{1}{c^2} \frac{\partial^2 E}{\partial t^2} = \frac{1}{\epsilon_0 c^2} \frac{\partial^2 P}{\partial t^2} \quad (2)$$

with the electric polarization intensity given by $P = \epsilon_0 \chi_D^{(1)} E + Neq_1$, where N the density of unit cells, e is the unit charge, and $\chi_D^{(1)}$ is the optical susceptibility of the background material (which is assumed to be linear). Note that the resonance of the two SRRs (dark mode) has no contribution to the average field E because the asymmetric field distribution at the two SRRs cancels each other when PIT occurs [8,16]. In addition, since the wavelength of the incident field (8.5 mm) is much larger than the thickness of each unit cell (10 μm), the electric field E seen by each meta-atom (i.e., the unit cell) is nearly homogeneous. Thus we can take an electric-dipole approximation, widely used in atomic physics and quantum optics [26], to investigate the dynamics of the system. In terms of the relation $P = \epsilon_0 \chi E$, the electric susceptibility χ can be obtained by the formula

$$\chi = \chi_D^{(1)} + \frac{Ne}{\epsilon_0 E} q_1. \quad (3)$$

To obtain the explicit expression of q_1 , we must solve the Maxwell-Lorentz (ML) equations (1) and (2). We assume the incident radiation has frequency ω_f , which is near ω_0 . Thus, there is resonant interaction between the electric field E and the oscillators q_1 and q_2 . To treat such resonant, nonlinear problem analytically, we assume $q_j = q_{dj} + (q_{fj} e^{i(k_0 z - \omega_0 t)} + \text{c.c.}) + (q_{sj} e^{2i(k_0 z - \omega_0 t)} + \text{c.c.})$, $E = E_d + (E_f e^{i(k_f z - \omega_f t)} + \text{c.c.}) + (E_s e^{i[(2k_f + \Delta k)z - 2\omega_f t]} + \text{c.c.})$. Here q_{dj} , q_{fj} , and q_{sj} are respectively amplitudes of the longwave (rectification field or mean field), shortwave (fundamental wave), and second harmonic wave of the j th oscillator, with k_0 (ω_0) the wave number (frequency) of the fundamental wave; E_d , E_f , and E_s are respectively amplitudes of the longwave, shortwave, and second harmonic wave of the electric field; k_f (ω_f) is the wave number (frequency) of the fundamental wave, and Δk is a detuning. Note that in the present work we only consider the longwave-shortwave resonance (a special three-wave resonance) of the gigahertz radiation. Other resonance processes, such as general three-wave resonance, will not be discussed. From the ML equations (1) and (2) and using rotating-wave and slowly varying envelope approximations, we can obtain a series of equations for the motion of $q_{\mu j}$ and E_μ ($\mu = d, f$), which are listed in Appendix A.

III. ENHANCED KERR NONLINEARITIES AND DS EQUATIONS

A. Asymptotic expansion and DS equations

We now investigate second- and third-order nonlinear susceptibilities, which can be used to generate the dromionlike nonlinear excitations through the longwave-shortwave resonant interaction in the system. To this end, we solve the equations for $q_{\alpha j}$ and E_α by using the method of multiple scales [27]. Take the asymptotic expansion $q_{fj} = \epsilon q_{fj}^{(1)} + \epsilon^2 q_{fj}^{(2)} + \dots$, $q_{dj} = \epsilon^2 q_{dj}^{(2)} + \dots$, $q_{sj} = \epsilon^2 q_{sj}^{(2)} + \dots$, $E_f = \epsilon E_f^{(1)} + \epsilon^2 E_f^{(2)} + \dots$, $E_d = \epsilon^2 E_d^{(2)} + \dots$, where ϵ is a

dimensionless small parameter characterizing the amplitude of the incident electric field. All quantities on the right-hand side of the expansion are assumed as functions of the multiscale variables $x_1 = \epsilon x$, $y_1 = \epsilon y$, $z_j = \epsilon^j z$ ($j = 0, 1, 2$), and $t_j = \epsilon^j t$ ($j = 0, 1$). Substituting this expansion into the equations for $q_{\mu j}$ and E_μ and comparing the expansion parameter of each power ϵ , we obtain a chain of linear but inhomogeneous equations (listed in Appendix B), which can be solved order by order.

At the first-order we obtain the solution for the shortwave field $E_f^{(1)} = F \exp[i(Kz_0 - \delta t_0)]$ where F is a yet to be determined envelope function depending on the slow variables x_1, y_1, z_1, z_2 , and t_1 , $\delta = \omega_f - \omega_0$ is frequency detuning, and K is the linear dispersion relation given by

$$K = \frac{n_D}{c} \delta + \frac{\kappa_0 g D_2(\delta)}{D_1(\delta) D_2(\delta) - \kappa^4}. \quad (4)$$

Here $D_j(l\delta) = \omega_0^2 - l^2(\omega_0 + \delta)^2 - il\gamma_j(\omega_0 + \delta)$ ($j, l = 1, 2$) and $\kappa_0 = (Ne\omega_0)/(2\epsilon_0 c n_D)$. Shown in Fig. 1(d) is the absorption spectrum $\text{Im}(K)$ (the imaginary part of K) as a function of the incident-wave frequency $\omega_f/(2\pi)$. When plotting the figure we used the damping rates $\gamma_1 \approx 60$ GHz and $\gamma_2 \approx 10$ GHz, which are nearly independent of d , whereas κ increases from 0 (sole CW) to 145.5 GHz at $d = 0.03$ mm. We see that the analytical result (blue dashed lines) fits well with the numerical one (orange solid lines). Solutions of bright and dark modes at this order read $q_{f1}^{(1)} = g D_2(\delta) E_f^{(1)} / [D_1(\delta) D_2(\delta) - \kappa^4]$, $q_{f2}^{(1)} = g \kappa^2 E_f^{(1)} / [D_1(\delta) D_2(\delta) - \kappa^4]$.

At the second order, a divergence-free condition requires $\partial F / \partial z_1 + (1/V_g) \partial F / \partial t_1 = 0$, where $V_g = (\partial K / \partial \delta)^{-1}$ is the group velocity of the shortwave envelope F . The solution for the longwave (rectification) field reads $E_d^{(2)} = G$, and explicit expressions for other quantities at this order are presented in Appendix C.

With the above results we proceed to the third order. The solvability condition at this order yields the nonlinear equation

$$i \frac{\partial F}{\partial z_2} - \frac{1}{2} K_2 \frac{\partial^2 F}{\partial \tau_1^2} + \frac{c}{2\omega_0 n_D} \left(\frac{\partial^2}{\partial x_1^2} + \frac{\partial^2}{\partial y_1^2} \right) F + \frac{\omega_0}{2cn_D} \chi^{(3)} |F|^2 \times F e^{-2\bar{\alpha} z_2} + \frac{m_1 \omega_0}{2cn_D} \chi^{(2)} G F = 0. \quad (5)$$

Here $\tau_1 = \epsilon \tau$ ($\tau \equiv t - z/V_g$), $\bar{\alpha} = \epsilon^{-2} \text{Im}(K)$ is the coefficient describing linear absorption, $K_2 = \partial^2 K / \partial \delta^2$ is the coefficient describing group-velocity dispersion, $m_1 \equiv |D_1(\delta) D_2(\delta) - \kappa^4|^2 / [D_1(\delta) D_2(\delta) - \kappa^4]^2$, $\chi^{(2)}$, and $\chi^{(3)}$ are, respectively, the second-order and third-order nonlinear susceptibilities with the form

$$\chi^{(2)} = \frac{-2N e g^2 \kappa^6 \alpha}{\epsilon_0 (\omega_0^4 - \kappa^4) |D_1(\delta) D_2(\delta) - \kappa^4|^2}, \quad (6a)$$

$$\chi^{(3)} = \left(\frac{4\alpha^2 \omega_0^2}{\omega_0^4 - \kappa^4} + \frac{2\alpha^2 D_1(2\delta)}{D_1(2\delta) D_2(2\delta) - \kappa^4} - 3\beta \right) \times \frac{g^3 \kappa^8 N e}{\epsilon_0 (D_1(\delta) D_2(\delta) - \kappa^4)^2 |D_1(\delta) D_2(\delta) - \kappa^4|^2}. \quad (6b)$$

We see that $\chi^{(2)}$ is proportional to the parameter α , i.e., it is contributed by the quadratic nonlinearity in Eq. (1b); $\chi^{(3)}$ is

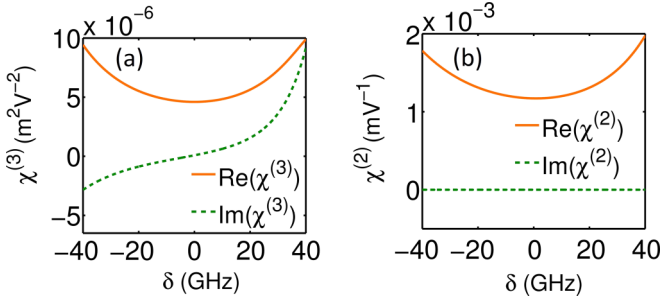


FIG. 2. Nonlinear susceptibilities of the PIT metamaterial. (a) Real and imaginary parts of the third-order susceptibility $\chi^{(3)}$ [i.e., $\text{Re}(\chi^{(3)})$ and $\text{Im}(\chi^{(3)})$] as functions of the frequency detuning δ . (b) Real and imaginary parts of the second-order susceptibility $\chi^{(2)}$ [i.e., $\text{Re}(\chi^{(2)})$ and $\text{Im}(\chi^{(2)})$] as functions of δ . System parameters used are given in the text.

proportional to the parameters β and α , which means that it comes from the contributions by the cubic nonlinearity (the term proportional to the parameter β) and by the quadratic nonlinearity (the terms proportional to the parameter α) in Eq. (1b).

Furthermore, the nonlinear equation for the longwave (rectification) field G arises at the fourth-order approximation, which reads

$$\left(\frac{\partial^2}{\partial x_1^2} + \frac{\partial^2}{\partial y_1^2} \right) G - \left(\frac{1}{V_p^2} - \frac{1}{V_g^2} \right) \frac{\partial^2 G}{\partial \tau_1^2} - \frac{\chi^{(2)}}{c^2} \frac{\partial^2 |F|^2}{\partial \tau_1^2} \times e^{-2\tilde{\alpha}z_2} = 0, \quad (7)$$

where V_p is the phase velocity of the longwave field G , defined by

$$\frac{1}{V_p^2} = \frac{n_D^2}{c^2} + \frac{N \text{eg} \omega_0^2}{\epsilon_0 c^2 (\omega_0^4 - \kappa^4)}. \quad (8)$$

The last term on the left-hand side of Eq. (7) corresponds to a second-order plasmonic rectification. Above results tell us that the self-interaction of the shortwave (with the envelope F) can stimulate the generation of the longwave field G [Eq. (7)], and at the same time longwave field G has a back-action to the shortwave field F [Eq. (5)]. Equations (5) and (7) are the general form of DS equations describing the propagation of high-dimensional nonlinear plasmonic polaritons in the system.

B. Enhanced Kerr effect due to the resonant interaction between longwave and shortwave

Since the nonlinear behavior of the high-dimensional plasmonic polaritons is determined by the combined action of the second-order and third-order nonlinear susceptibilities, it is necessary to give a detailed discussion on them. For this aim, in Fig. 2(a) and Fig. 2(b) we show, respectively, curves of $\chi^{(3)}$ and $\chi^{(2)}$ as functions of the frequency detuning δ , in which the orange solid lines are their real parts and the green dashed lines are their imaginary parts. From the figure we can obtain the following conclusions: (i) $\chi^{(2)}$ is nearly real [i.e., $\text{Im}(\chi^{(2)}) \approx 0$] and has the order of magnitude 10^{-3} mV^{-1} . (ii) the real part of the third-order susceptibility, $\text{Re}(\chi^{(3)})$, has the order of magnitude $10^{-6} \text{ m}^2\text{V}^{-2}$. The physical reason

for such large second- and third-order nonlinearities predicted here is due to the fact that the incident radiation E is resonant with the oscillators q_1 , q_2 and the system works under the PIT condition. (iii) The imaginary part of $\chi^{(3)}$ [i.e., $\text{Im}(\chi^{(3)})$], which contributes a nonlinear absorption to the radiation field, is much less than the real part $\text{Re}(\chi^{(3)})$ when the system works in the PIT transparency window (i.e., δ takes values within the interval from -20 GHz to 20 GHz). Such suppression of the nonlinear absorption is also due to the PIT effect.

Interestingly, the third-order nonlinear susceptibility $\chi^{(3)}$ can be further enhanced by using longwave-shortwave resonance. This can be seen from the following analysis. For simplicity but without loss of generality of the analysis of nonlinear susceptibilities, we assume that the transverse spatial distribution of the radiation is large enough so that the diffraction effect (i.e., its dependence on the transverse coordinates x and y) of the system can be neglected. Then from Eq. (7) we obtain $G = \chi^{(2)} |E_f|^2 / [c^2 (1/V_g^2 - 1/V_p^2)]$. Plugging this result into Eq. (5), we obtain an effective third-order nonlinear susceptibility

$$\chi_{\text{eff}}^{(3)} = \chi^{(3)} + \chi_{\text{SL}}^{(3)}, \quad (9a)$$

$$\chi_{\text{SL}}^{(3)} = m_1 \frac{(\chi^{(2)})^2}{c^2 \left(\frac{1}{V_p^2} - \frac{1}{V_g^2} \right)}, \quad (9b)$$

where the subscript ‘‘SL’’ means that the corresponding term is due to the longwave-shortwave interaction. Equation (9) tells us that if some region of system parameters can be found where $V_p \approx V_g$, in addition to the PIT enhancement (i.e., $\chi^{(3)}$ is large, as shown in Fig. 2), the effective third-order nonlinear susceptibility $\chi_{\text{eff}}^{(3)}$ can be further enhanced because of the drastic enhancement of $\chi_{\text{SL}}^{(3)}$.

In the situation $V_p \approx V_g$, the system undergoes a resonant interaction between the longwave G and the shortwave F , a special form of three-wave resonance satisfying the conditions $\omega_1 + \omega_2 = \omega_3$ and $k_f(\omega_1) + k_f(\omega_2) = k_f(\omega_3)$. This point can be illustrated clearly if we choose $\omega_1 = \omega - \epsilon\delta$, $\omega_2 = 2\epsilon\delta$, and $\omega_3 = \omega + \epsilon\delta$. Then one has $\omega_1 + \omega_2 = \omega_3$, and $k_f(\omega_1) + k_f(\omega_2) - k_f(\omega_3) = k_f(\omega - \epsilon\delta) + k_f(2\epsilon\delta) - k_f(\omega + \epsilon\delta) = -2\epsilon\delta \partial k_f / \partial \omega + k_f(2\epsilon\delta) + O(\epsilon^3)$ which is zero to order ϵ^3 if $\partial k_f / \partial \omega \simeq k_f(2\epsilon\delta) / 2\epsilon\delta$, i.e., $V_g \simeq V_p$ [22].

In our system, a broad parameter region for $V_p \approx V_g$ exists. Illustrated in Fig. 3(a) is the denominator $1/V_p^2 - 1/V_g^2$ of $\chi_{\text{SL}}^{(3)}$ as functions of the frequency detuning δ and the coupling coefficient κ [see Eqs. (1)]. The rectangle enclosed by purple dashed lines in upper part of the figure illustrates the parameter region where $V_g \approx V_p$. Consequently, the longwave-shortwave resonance can indeed occur in the present PIT metamaterial, and based on this the effective third-order nonlinear susceptibility $\chi_{\text{eff}}^{(3)}$ of the system can be enhanced greatly.

Shown in Fig. 3(b) are curves of the real part $\text{Re}(\chi_{\text{eff}}^{(3)})$ (orange solid line) and the imaginary part $\text{Im}(\chi_{\text{eff}}^{(3)})$ (green dashed line) of the effective third-order nonlinear susceptibility $\chi_{\text{eff}}^{(3)}$ as functions of δ for $\kappa = 180$ GHz. We observe that $\text{Re}(\chi_{\text{eff}}^{(3)})$ [which is much larger $\text{Im}(\chi_{\text{eff}}^{(3)})$ near $\delta = 0$] is enhanced one order of magnitude (up to the value $6.64 \times 10^{-5} \text{ m}^2\text{V}^{-2}$),

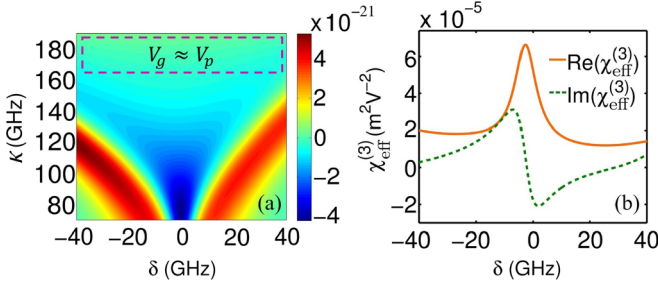


FIG. 3. (a) The denominator $1/V_p^2 - 1/V_g^2$ of $\chi_{\text{SL}}^{(3)}$ as functions of frequency detuning δ and the coupling coefficient κ . System parameters used are given in the text. The rectangle enclosed by purple dashed lines shows the region where the longwave-shortwave resonance occurs (i.e., $V_g \approx V_p$). (b) Real part $\text{Re}(\chi_{\text{eff}}^{(3)})$ (orange solid line) and imaginary part $\text{Im}(\chi_{\text{eff}}^{(3)})$ (green dashed line) of the effective third-order nonlinear susceptibility $\chi_{\text{eff}}^{(3)}$ as functions of frequency detuning δ for $\kappa = 180$ GHz.

which is contributed by the longwave-shortwave resonance interaction.

When plotting Fig. 2 and Fig. 3, the system parameters used are $\gamma_1 = 60$ GHz, $\gamma_2 = 10$ GHz, $g = 1.79 \times 10^{11}$ C kg $^{-1}$, $\kappa_0 = 2.8 \times 10^{-8}$ kg C $^{-1}$ cm $^{-1}$ GHz 2 , obtained by fitting the numerical result given in Fig. 1(d). The parameters α and β , introduced in Eq. (1b) for describing the nonlinear property of the hyperabrupt tuning varactors mounted onto the gaps of SRRs [23], have been elaborated in detail in Appendix D, which read $\alpha = -1.27 \times 10^{15}$ cm $^{-1}$ GHz 2 and $\beta = 2.26 \times 10^{25}$ cm $^{-2}$ GHz 2 .

IV. PLASMON DROMIONS

Now we turn to the formation and propagation of high-dimensional nonlinear plasmon polaritons in the system by examining possible dromion solutions of the Eq. (5) and Eq. (7). After returning to original variables and converting them into dimensionless forms, Eq. (5) and Eq. (7) become

$$i \frac{\partial u}{\partial s} + \left(\frac{\partial^2}{\partial \xi^2} + g_y \frac{\partial^2}{\partial \eta^2} + g_{d1} \frac{\partial^2}{\partial \sigma^2} \right) u + 2g_1 |u|^2 u + g_2 v u = -i d_0 u, \quad (10a)$$

$$g_{d2} \frac{\partial^2 v}{\partial \sigma^2} - \left(\frac{\partial^2}{\partial \xi^2} + g_y \frac{\partial^2}{\partial \eta^2} \right) v + g_3 \frac{\partial^2 |u|^2}{\partial \sigma^2} = 0, \quad (10b)$$

where $u = \epsilon F \exp(-\tilde{\alpha} z_2) / U_0$, $v = \epsilon^2 G / V_0$, $s = z / (2L_{\text{Diff}})$, $\sigma = (t - z / \tilde{V}_g) / \tau_0$, $\xi = x / R_x$, $\eta = y / R_y$, $g_y = (R_x / R_y)^2$, $g_{d1} = L_{\text{Diff}} / L_{\text{Disp}}$, $g_{d2} = R_x^2 (1 / V_p^2 - 1 / V_g^2) / \tau_0^2$, $g_1 = L_{\text{Diff}} / L_{\text{Nonl}}$, $g_2 = L_{\text{Diff}} m_1 \omega_0 V_0 \chi^{(2)} / (c n_D)$, $g_3 = \chi^{(2)} R_x^2 U_0^2 / (c^2 \tau_0^2 V_0)$, and $d_0 = 2L_{\text{Diff}} / L_A$. Here R_x (R_y) is typical radius of the incident pulse in x (y) direction, τ_0 is typical temporal length of the incident pulse; U_0 and V_0 are respectively amplitudes of the shortwave envelope and the longwave; $L_{\text{Disp}} = -\tau_0^2 / \tilde{K}_2$, $L_{\text{Diff}} = \omega_0 n_D R_x / c$, $L_{\text{Nonl}} = 2c n_D / [\omega_0 \tilde{\chi}^{(3)} U_0^2]$, and $L_A = 1 / \text{Im}(K)$ are respectively typical dispersion length, diffraction length, nonlinear length, and absorption length (the tilde above corresponding quantity means taking its real part). Note that when obtaining Eq. (10) we have neglected the imaginary parts of K_2 and $\chi^{(3)}$. This is reasonable because

the system works under the PIT condition $\kappa^2 \gg \omega_0 \sqrt{\gamma_1 \gamma_2}$ so that their imaginary parts are much smaller than their real parts.

Expressions (10a) and (10b) are coupled (3+1)D nonlinear partial differential equations including effects of dispersion, diffraction, nonlinearity, and a small loss caused by $\text{Im}(K)$. Because a general consideration to obtain stable high-dimensional nonlinear solutions of such equations is not available yet, here we consider only a specific case to seek possible (2+1)D dromion solutions by using some assumptions for simplification. First, we assume L_{Disp} , L_{Diff} , and L_{Nonl} have the same order of magnitude, which can be achieved by taking $\tau_0 = \sqrt{-\omega_0 n_D \tilde{K}_2 / c R_x}$ and $U_0 = \sqrt{2c^2 n_D / (\omega_0^2 n_D R_x^2 \tilde{\chi}^{(3)})}$. Second, we choose realistic system parameters $\delta = -10$ GHz, $R_x = 0.47$ cm, $R_y = 2.5$ cm, $\tau_0 = 2.21 \times 10^{-11}$ s, $V_0 = 0.51$ V cm $^{-1}$, $\alpha = -3.99 \times 10^{14}$ cm $^{-1}$ GHz 2 , $\beta = 4.36 \times 10^{25}$ cm $^{-2}$ GHz 2 , $\kappa = 198$ GHz. Then we obtain $L_{\text{Diff}} (= L_{\text{Disp}} = L_{\text{Nonl}}) = 4.99$ cm, $d_0 = 0.064$, $U_0 = 4.57$ V cm $^{-1}$, and $g_{d1} = g_1 = g_2 = g_{d2} = 1$, $g_3 = 4$, $g_y \approx 0$. In order to have $L_{\text{Nonl}} = 4.99$ cm, 22 layers or more of the unit cell array are needed. Because d_0 is small, the term on the right-hand side of Eq. (10a) can be taken as a perturbation. As a first step, we neglect such perturbation and hence Eq. (10a) and Eq. (10b) are simplified into standard Davey-Stewartson-I (DSI) equations

$$i \frac{\partial u}{\partial s} + \frac{\partial^2 u}{\partial \sigma^2} + \frac{\partial^2 u}{\partial \xi^2} + 2|u|^2 u + v u = 0, \quad (11a)$$

$$\frac{\partial^2 v}{\partial \sigma^2} - \frac{\partial^2 v}{\partial \xi^2} + 4 \frac{\partial^2 |u|^2}{\partial \sigma^2} = 0, \quad (11b)$$

which are completely integrable and can be solved exactly by the use of inverse scattering transform. One of remarkable properties of the DSI equations is that they allow various dromion solutions [28]. A single dromion solution of the DSI equations reads $u = Q/P$, $v = 4\partial^2 \ln P / \partial \sigma^2$, where $P = 1 + \exp(\eta_1 + \eta_1^*) + \exp(\eta_2 + \eta_2^*) + \gamma \exp(\eta_1 + \eta_1^* + \eta_2 + \eta_2^*)$ and $Q = \rho \exp(\eta_1 + \eta_2)$, with $\eta_1 = (k_r + i k_i)(\xi + \sigma) / \sqrt{2} + (\Omega_r + i \Omega_i)s$, $\eta_2 = (l_r + i l_i)(\xi - \sigma) / \sqrt{2} + (\omega_r + i \omega_i)s$, $\Omega_r = -2k_r k_i$, $\omega_r = -2l_r l_i$, $\Omega_i + \omega_i = k_r^2 + l_r^2 - k_i^2 - l_i^2$, $\rho = |\rho| \exp(i \varphi_\rho)$, and $|\rho| = 2[2k_r l_r (\gamma - 1)]^{1/2}$. Here, k_r , k_i , l_r , l_i , $|\rho|$, φ_ρ , and γ are real integration constants. If we choose $k_r, l_r > 0$, we have $\gamma = \exp(2\varphi_\gamma)$ with $\varphi_\gamma > 0$. By taking $k_r = \sqrt{2}\mu$, $k_i = \sqrt{2}a_1$, $l_r = \sqrt{2}\lambda$, $l_i = \sqrt{2}p$ ($\lambda\mu \geq 0$), $\Omega_i = 2(\mu^2 - a_1^2)$, $\omega_i = 2(\lambda^2 - p^2)$, $\Omega_r = -4a\mu$, and $\omega_r = -4\lambda p$, we obtain explicit expressions

$$u = \frac{2\mu \exp(ih)}{m \cosh f_1 + n \cosh f_2}, \quad (12a)$$

$$v = \frac{4(m^2 + n^2)(\mu^2 + \lambda^2) - 8\mu^2}{(m \cosh f_1 + n \cosh f_2)^2} + \frac{8mn[(\mu^2 + \lambda^2) \cosh f_1 \cosh f_2 - (\mu^2 - \lambda^2) \sinh f_1 \sinh f_2]}{(m \cosh f_1 + n \cosh f_2)^2}, \quad (12b)$$

where $m = \{\mu / [\lambda(\gamma - 1)]\}^{1/2}$, $n = \{\mu\gamma / [\lambda(\gamma - 1)]\}^{1/2}$, $h = a_1(\sigma + \xi) + p(\sigma - \xi) + 2(\mu^2 + \lambda^2 - a_1^2 - p^2)s + \varphi_\rho$, $f_1 =$

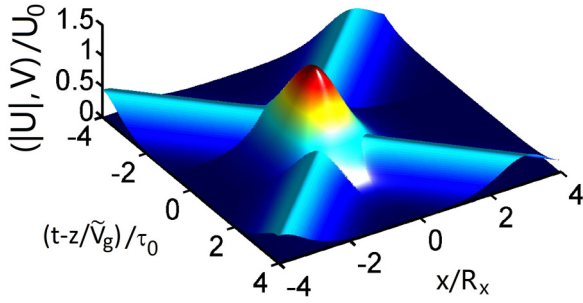


FIG. 4. A single dromion excitation in the PIT metamaterial, which consists of a localized envelope for the shortwave component and two tracks for the longwave component. Plotted here is the shortwave envelope $|u| = |U|/U_0$ (the hump at the center) and the longwave (rectification) field $v = V/U_0$ [the two crossed tracks (plane solitons)] as functions of $\xi = x/R_x$ and $\sigma = (t - z/\tilde{V}_g)/\tau_0$. System parameters are chosen as $\mu = 1$, $\lambda = 1$, $a_1 = 0$, $p = 0$, $\varphi_\rho = 0$, $\varphi_\gamma = 0$ at $s = 0$.

$\mu(\sigma + \xi) - \lambda(\sigma - \xi) - 4(a_1\mu - \lambda p)s$, $f_2 = \mu(\sigma + \xi) + \lambda(\sigma - \xi) - 4(a_1\mu + \lambda p)s + \varphi_\gamma$. Obviously, the dromion given above consists of a localized envelope u for the shortwave component, which decays exponentially in all spatial directions (shown by the hump at the center of Fig. 4), and two plane solitons for the longwave component v , in which each plane soliton decays in its traveling direction (shown by the two tracks in Fig. 4).

The result presented above is the dromion solution based on Eq. (11a) and Eq. (11b) without considering the loss (although it is small under the PIT condition) in the system. It is necessary to investigate the spatiotemporal evolution of the dromion and its stability starting directly from Eq. (5) and Eq. (7). For this aim, we make a numerical simulation on Eq. (5) and Eq. (7) by taking the dromion solution (12) with a random disturbance as an initial condition. Concretely, we take $U(z = 0, x, t) = U_0 u \times (1 + \varepsilon f_R)$, with u being the dromion solution (12), ε being a typical amplitude of the perturbation, and f_R being a random variable uniformly distributed in the interval $[0, 1]$. Shown in Fig. 5 is the evolution of the dromion pulse as a function of $\xi = x/R_x$ and $\sigma = (t - z/\tilde{V}_g)/\tau_0$ by taking $\varepsilon = 0.1$. The profiles from Figs. 5(a)–5(e) in the figure are respectively for the propagation distance $z = 0, 0.5L_{\text{Diff}}, L_{\text{diff}}, 1.5L_{\text{diff}}$, and $2L_{\text{diff}}$, with $L_{\text{Diff}} = 4.99$ cm. We see that the shape of the dromion undergoes no apparent change, but its amplitude is reduced a little during propagation due to the small loss inherent in the dark oscillator q_2 .

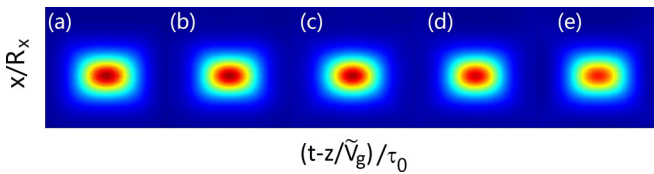


FIG. 5. Spatiotemporal evolution of the plasmon dromion as a function of $\xi = x/R_x$ and $\sigma = (t - z/\tilde{V}_g)/\tau_0$ based on Eq. (5) and Eq. (7), by taking the solution (12) plus 10% random disturbance as an initial condition. (a) Initial profile of the dromion ($z = 0$). (b), (c), (d), and (e) are dromion profiles when propagating respectively to $z = 0.5L_{\text{Diff}}, 1.0L_{\text{Diff}}, 1.5L_{\text{Diff}}, 2.0L_{\text{Diff}}$, with $L_{\text{Diff}} = 4.99$ cm.

The threshold of the power density of the incident radiation \bar{P}_{peak} for generating the plasmon dromion given above can be estimated by using Poyntings vector [22]. With our system parameters, the average peak power of the plasmon dromion is

$$\bar{P}_{\text{peak}} = 814 \text{ mW}, \quad (13)$$

which corresponds average peak intensity $\bar{I}_{\text{peak}} = 361 \text{ mW/cm}^2$. We see that in the PIT metamaterial extremely low generation power is needed for generating (2+1)D spatiotemporal dromions.

V. CONCLUSIONS

In this article, we have proposed a scheme to realize a giant Kerr nonlinearity and create stable (2+1)D nonlinear plasmon polaritons via PIT in a metamaterial. We have shown that, due to the PIT effect and the nonlinearity contributed by the varactor the system can possess very large second-order and third-order nonlinear susceptibilities. We have further shown that the effective third-order nonlinear susceptibility $\chi_{\text{eff}}^{(3)}$ can be further enhanced one order of magnitude (up to $6.8 \times 10^{-5} \text{ m}^2 \text{V}^{-2}$) through the resonant interaction between longwave and shortwave, which happens when $V_p \approx V_g$ and is shown to be possible in our system. Based on these important properties in the proposed system, we have derived the Davey-Stewartson (DS) equations, which govern the evolution of longwave and shortwave envelope, and demonstrated that it possible to generate plasmon dromions with very low generation power. Our study raises the possibility for obtaining giant Kerr effect and stable high-dimensional nonlinear plasmon polaritons at rather low radiation intensity by the use of nonlinear PIT metamaterials.

ACKNOWLEDGMENTS

This work was supported by the NSF-China under Grants No. 11174080 and No. 11474099, and by the Chinese Education Ministry Reward for Excellent Doctors in Academics under Grant No. PY2014009.

APPENDIX A: EQUATIONS FOR $q_{\mu j}$ AND E_μ BASED ON THE MAXWELL-LORENTZ EQUATIONS

Equations of motion of the oscillators $q_{\mu j}$ read

$$\ddot{q}_{f1} + (\gamma_1 - 2i\omega_0)\dot{q}_{f1} - i\gamma_1\omega_0q_{f1} - \kappa^2q_{f2} = gE_f, \quad (\text{A1a})$$

$$\ddot{q}_{f2} + (\gamma_2 - 2i\omega_0)\dot{q}_{f2} - i\gamma_2\omega_0q_{f2} - \kappa^2q_{f1} + 2\alpha q_{d2}q_{f2} + 3\beta|q_{f2}|^2q_{f2} = 0, \quad (\text{A1b})$$

$$\ddot{q}_{d1} + \gamma_1\dot{q}_{d1} + \omega_0^2q_{d1} - \kappa^2q_{d2} = gE_d, \quad (\text{A1c})$$

$$\ddot{q}_{d2} + \gamma_2\dot{q}_{d2} + \omega_0^2q_{d2} - \kappa^2q_{d1} + 2\alpha|q_{f2}|^2 = 0, \quad (\text{A1d})$$

$$\ddot{q}_{s1} + (\gamma_1 - 4i\omega_0)\dot{q}_{s1} + (\omega_0^2 - 2i\gamma_1\omega_0 - 4\omega_0^2)q_{s1} - \kappa^2q_{s2} = gE_s e^{i\Delta kz}, \quad (\text{A1e})$$

$$\ddot{q}_{s2} + (\gamma_2 - 4i\omega_0)\dot{q}_{s2} + (\omega_0^2 - 2i\gamma_2\omega_0 - 4\omega_0^2)q_{s2} - \kappa^2q_{s1} + \alpha q_{f2}^2 = 0. \quad (\text{A1f})$$

The equation of motion for electric field E_μ are given by

$$i\left(\frac{\partial}{\partial z} + \frac{n_D}{c} \frac{\partial}{\partial t}\right)E_f + \frac{c}{2\omega_0 n_D} \left(\frac{\partial^2}{\partial x^2} + \frac{\partial^2}{\partial y^2}\right)E_f + \kappa_0 q_{f1} = 0, \quad (\text{A2a})$$

$$\left(\frac{\partial^2}{\partial x^2} + \frac{\partial^2}{\partial y^2} + \frac{\partial^2}{\partial z^2}\right)E_d - \frac{n_D^2}{c^2} \frac{\partial^2}{\partial t^2} E_d = \frac{Ne}{\varepsilon_0 c^2} \frac{\partial^2}{\partial t^2} q_{d1}, \quad (\text{A2b})$$

$$i\left(\frac{\partial}{\partial z} + \frac{n_D}{c} \frac{\partial}{\partial t}\right)E_s + \frac{c}{4\omega_0 n_D} \left(\frac{\partial^2}{\partial x^2} + \frac{\partial^2}{\partial y^2}\right)E_s + 2\kappa_0 q_{s1} e^{-i\Delta kz} = 0, \quad (\text{A2c})$$

where $n_D = \sqrt{1 + \chi_D^{(1)}}$, and $\kappa_0 = (Ne\omega_0)/(2\varepsilon_0 c n_D)$.

APPENDIX B: ASYMPTOTIC EXPANSION OF THE MAXWELL-LORENTZ EQUATIONS

The asymptotic expansions of the equations of motion for $q_{\mu j}$ read

$$\frac{\partial^2}{\partial t_0^2} q_{f1}^{(l)} + (\gamma_1 - 2i\omega_0) \frac{\partial}{\partial t_0} q_{f1}^{(l)} - i\gamma_1 \omega_0 q_{f1}^{(l)} - \kappa^2 q_{f1}^{(l)} - g E_f^{(l)} = A^{(l)}, \quad (\text{B1a})$$

$$\frac{\partial^2}{\partial t_0^2} q_{f2}^{(l)} + (\gamma_2 - 2i\omega_0) \frac{\partial}{\partial t_0} q_{f2}^{(l)} - i\gamma_2 \omega_0 q_{f2}^{(l)} - \kappa^2 q_{f1}^{(l)} = B^{(l)}, \quad (\text{B1b})$$

$$\frac{\partial^2}{\partial t_0^2} q_{d1}^{(l)} + \gamma_1 \frac{\partial}{\partial t_0} q_{d1}^{(l)} + \omega_0^2 q_{d1}^{(l)} - \kappa^2 q_{d2}^{(l)} - g E_d^{(l)} = C^{(l)}, \quad (\text{B1c})$$

$$\frac{\partial^2}{\partial t_0^2} q_{d2}^{(l)} + \gamma_2 \frac{\partial}{\partial t_0} q_{d2}^{(l)} + \omega_0^2 q_{d2}^{(l)} - \kappa^2 q_{d1}^{(l)} = D^{(l)}, \quad (\text{B1d})$$

$$\frac{\partial^2}{\partial t_0^2} q_{s1}^{(l)} + (\gamma_1 - 4i\omega_0) \frac{\partial}{\partial t_0} q_{s1}^{(l)} + (\omega_0^2 - 2i\gamma_1 \omega_0 - 4\omega_0^2) q_{s1}^{(l)} - \kappa^2 q_{s2}^{(l)} = E^{(l)}, \quad (\text{B1e})$$

$$\frac{\partial^2}{\partial t_0^2} q_{s2}^{(l)} + (\gamma_2 - 4i\omega_0) \frac{\partial}{\partial t_0} q_{s2}^{(l)} + (\omega_0^2 - 2i\gamma_2 \omega_0 - 4\omega_0^2) q_{s2}^{(l)} - \kappa^2 q_{s1}^{(l)} = F^{(l)}. \quad (\text{B1f})$$

The asymptotic expansion of the Maxwell equation is

$$i\left(\frac{\partial}{\partial z_0} + \frac{n_D}{c} \frac{\partial}{\partial t_0}\right)E_f^{(l)} + \kappa_0 q_{f1}^{(l)} = M^{(l)}, \quad (\text{B2a})$$

$$\frac{\partial^2}{\partial z_0^2} E_d^{(l)} - \frac{n_D^2}{c^2} \frac{\partial^2}{\partial t_0^2} E_d^{(l)} - \frac{Ne}{\varepsilon_0 c^2} \frac{\partial^2}{\partial t_0^2} q_{d1}^{(l)} = N^{(l)}. \quad (\text{B2b})$$

The quantities on the right-hand side of Eqs. (B1) and (B2) are given by $A^{(1)} = B^{(1)} = C^{(1)} = D^{(1)} = E^{(1)} = F^{(1)} = M^{(1)} = N^{(1)} = C^{(2)} = E^{(2)} = N^{(2)} = N^{(3)} = 0$, $A^{(2)} = -2\partial^2 q_{f1}^{(1)}/\partial t_0 \partial t_1 - (\gamma_1 - 2i\omega_0) \partial q_{f1}^{(1)}/\partial t_1$, $B^{(2)} = -2\partial^2 q_{f2}^{(1)}/\partial t_0 \partial t_1 - (\gamma_2 - 2i\omega_0) \partial q_{f2}^{(1)}/\partial t_1$, $D^{(2)} = -2\alpha |q_{f2}^{(1)}|^2$, $F^{(2)} = -\alpha (q_{f2}^{(1)})^2$, $M^{(2)} = -i[\partial/\partial z_1 + (n_D/c)\partial/\partial t_1]E_f^{(1)}$, $A^{(3)} = -2\partial^2 q_{f1}^{(2)}/\partial t_0 \partial t_1 - \partial^2 q_{f1}^{(1)}/\partial t_1^2 - (\gamma_1 - 2i\omega_0) \partial q_{f1}^{(2)}/\partial t_1$, $B^{(3)} = -2\partial^2 q_{f2}^{(2)}/\partial t_0 \partial t_1 - \partial^2 q_{f2}^{(1)}/\partial t_1^2 - (\gamma_2 - 2i\omega_0) \partial q_{f2}^{(2)}/\partial t_1$, $C^{(3)} = -2\partial^2 q_{d1}^{(2)}/\partial t_0 \partial t_1 - \partial^2 q_{d1}^{(1)}/\partial t_1^2 - (\gamma_1 - 2i\omega_0) \partial q_{d1}^{(2)}/\partial t_1$, $D^{(3)} = -2\partial^2 q_{d2}^{(2)}/\partial t_0 \partial t_1 - \partial^2 q_{d2}^{(1)}/\partial t_1^2 - (\gamma_2 - 2i\omega_0) \partial q_{d2}^{(2)}/\partial t_1$, $E^{(3)} = -2\partial^2 q_{s1}^{(2)}/\partial t_0 \partial t_1 - \partial^2 q_{s1}^{(1)}/\partial t_1^2 - (\gamma_1 - 4i\omega_0) \partial q_{s1}^{(2)}/\partial t_1$, $F^{(3)} = -2\partial^2 q_{s2}^{(2)}/\partial t_0 \partial t_1 - \partial^2 q_{s2}^{(1)}/\partial t_1^2 - (\gamma_2 - 4i\omega_0) \partial q_{s2}^{(2)}/\partial t_1$.

$$\partial t_0 \partial t_1 - \partial^2 q_{f2}^{(1)}/\partial t_1^2 - (\gamma_2 - 2i\omega_0) \partial q_{f2}^{(2)}/\partial t_1 - 2\alpha q_{d2}^{(2)} q_{f2}^{(1)} - 3\beta |q_{f2}^{(1)}|^2 q_{f2}^{(1)}, \quad M^{(3)} = -i[\partial/\partial z_1 + (n_D/c)\partial/\partial t_1]E_f^{(2)} - c/(2n_D \omega_0)(\partial^2/\partial x_1^2 + \partial^2/\partial y_1^2)E_f - i\partial E_f^{(1)}/\partial z_2, \quad \text{and } N^{(4)} = -(\partial^2/\partial x_1^2 + \partial^2/\partial y_1^2 + \partial^2/\partial z_1^2)E_d^{(2)} + (n_D/c)^2 \partial^2 E_d^{(2)}/\partial t_1^2 + Ne/(\varepsilon_0 c^2) \partial^2 q_{d1}^{(2)}/\partial t_1^2.$$

APPENDIX C: EXPLICIT EXPRESSIONS OF THE SECOND-ORDER SOLUTIONS

The second-order solution reads

$$q_{f1}^{(2)} = \frac{g D_2(\delta)^2 [2i(\omega_0 + \delta) - \gamma_1] + g \kappa^4 [2i(\omega_0 + \delta) - \gamma_2]}{(D_1(\delta) D_2(\delta) - \kappa^4)^2} \times \frac{\partial F}{\partial t_1} e^{i(Kz_0 - \delta t_0)}, \quad (\text{C1a})$$

$$q_{f2}^{(2)} = \frac{g \kappa^2 D_1(\delta) [2i(\omega_0 + \delta) - \gamma_2] + g \kappa^2 D_2(\delta) [2i(\omega_0 + \delta) - \gamma_1]}{(D_1(\delta) D_2(\delta) - \kappa^4)^2} \times \frac{\partial F}{\partial t_1} e^{i(Kz_0 - \delta t_0)}, \quad (\text{C1b})$$

$$q_{d1}^{(2)} = \frac{\omega_0^2 g G}{\omega^4 - \kappa^4} - \frac{2g^2 \kappa^6 \alpha}{(\omega_0^4 - \kappa^4) |D_1(\delta) D_2(\delta) - \kappa^4|^2} |F|^2 e^{-2\bar{\alpha} z_2}, \quad (\text{C1c})$$

$$q_{d2}^{(2)} = \frac{g \kappa^2 G}{\omega_0^2 - \kappa^4} - \frac{2\alpha \omega_0^2 g^2 \kappa^4}{(\omega_0^4 - \kappa^4) |D_1(\delta) D_2(\delta) - \kappa^4|^2} |F|^2 e^{-2\bar{\alpha} z_2}, \quad (\text{C1d})$$

$$q_{s1}^{(2)} = -\frac{g^2 \kappa^6 \alpha}{[D_1(\delta) D_2(\delta) - \kappa^4]^2 [D_1(2\delta) D_2(2\delta) - \kappa^4]} \times F^2 e^{2i(Kz_0 - \delta t_0)}, \quad (\text{C1e})$$

$$q_{s2}^{(2)} = -\frac{\alpha g^2 \kappa^4 D_1(2\delta)}{[D_1(\delta) D_2(\delta) - \kappa^4]^2 [D_1(2\delta) D_2(2\delta) - \kappa^4]} \times F^2 e^{2i(Kz_0 - \delta t_0)}. \quad (\text{C1f})$$

APPENDIX D: CALCULATION OF NONLINEAR COEFFICIENTS α AND β IN EQ. (1b)

The nonlinear property of the SRRs with mounted hyperabrupt tuning varactors has been theoretically analyzed and experimentally measured in Ref. [23]. The hyperabrupt tuning varactors provide a nonlinear voltage-dependent capacitance $C(V)$, which can be described by the expression $C(V) = C_0(1 - V/\bar{V})^{-M}$, where C_0 is the dc rest capacitance, \bar{V} is the intrinsic potential, and M is a dimensionless number less than one. From the definition $C(V) = dQ/dV$ (Q is electric charge), the voltage V across the varactors can be expressed as a function of q , i.e., $V(q) = \bar{V}[1 - (1 - q \frac{1-M}{\bar{V}})^{\frac{1}{1-M}}]$, where $q = Q/C_0$ is renormalized voltage. Expanding $V(q)$ by a Taylor series for a small oscillation (with the oscillation amplitude satisfying $(1 - M)|q| < \bar{V}$), one has $V(q) \approx q - M/(2\bar{V})q^2 + M(2M - 1)/(6\bar{V}^2)q^3$ when keeping to the third-order approximation. As a result, we obtain the second- and third-order nonlinear coefficients, given, respectively, by $-M/(2\bar{V})$ and $M(2M - 1)/(6\bar{V}^2)$.

The value of q in Ref. [23] (the renormalized voltage) has the dimension of volt, while the value of q_2 in our model (the amplitude of the dark mode) has the dimension of centimeter with the order of magnitude around 10^{-10} cm based on our analytical result. To make a comparison we switch the dimension of our Eq. (1a) and Eq. (1b), which reads

$$\ddot{x}_1 + \gamma_1 \dot{x}_1 + \omega_0^2 x_1 - \kappa^2 x_2 = \frac{g}{Q_0} E, \quad (\text{D1})$$

$$\ddot{x}_2 + \gamma_2 \dot{x}_2 + (\omega_0 + \Delta)^2 x_2 - \kappa^2 x_1 + Q_0 \alpha x_2^2 + Q_0^2 \beta x_2^3 = 0, \quad (\text{D2})$$

where $q_j = Q_0 x_j$ ($j = 1, 2$). x_j has the dimension of volt with the order of magnitude around 10 V, Q_0 has the dimension cm V^{-1} with the order of magnitude around 10^{-11} cm V^{-1} . Thus, nonlinear coefficients α and β in Eq. (1a) and Eq. (1b) can be calculated by using the expressions of $\alpha = Q_0^{-1} M_1 (\omega_0 + \Delta)^2$ and $\beta = Q_0^{-2} M_2 (\omega_0 + \Delta)^2$, where $M_1 = -M/(2\bar{V})$ and $M_2 = M(2M - 1)/(6\bar{V}^2)$. Choosing $Q_0 = 1.2 \times 10^{-11}$ cm V^{-1} , $M = 0.9$, $\bar{V} = 1.3\text{V}$, and using $(\omega_0, \Delta) = (2\pi \times 32, 8)$ GHz, we obtain $\alpha = -1.27 \times 10^{15}$ cm^{-1} GHz^2 and $\beta = 2.26 \times 10^{25}$ cm^{-2} GHz^2 .

-
- [1] M. Fleischhauer, A. Imamoglu, and J. P. Marangos, Electromagnetically induced transparency: Optics in coherent media, *Rev. Mod. Phys.* **77**, 633 (2005).
- [2] C. L. G. Alzar, M. A. G. Martinez, and P. Nussenzeivg, Classical analog of electromagnetically induced transparency, *Am. J. Phys.* **70**, 37 (2002).
- [3] J. Harden, A. Joshi, and J. D. Serna, Demonstration of double EIT using coupled harmonic oscillators and RLC circuits, *Eur. J. Phys.* **32**, 541 (2011).
- [4] J. A. Souza, L. Cabral, R. R. Oliveira, and C. J. Villas-Boas, Electromagnetically-induced-transparency-related phenomena and their mechanical analogs, *Phys. Rev. A* **92**, 023818 (2015).
- [5] S. Weis, R. Rivière, S. Deléglise, E. Gavartin, O. Arcizet, A. Schliesser, and T. J. Kippenberg, Optomechanically induced transparency, *Science* **330**, 1520 (2010).
- [6] A. Kronwald and F. Marquardt, Optomechanically Induced Transparency in the Nonlinear Quantum Regime, *Phys. Rev. Lett.* **111**, 133601 (2013).
- [7] B. Peng, S. K. Özdemir, W. Chen, F. Nori, and L. Yang, What is and what is not electromagnetically induced transparency in whispering-gallery microcavities, *Nature Commun.* **5**, 5082 (2014).
- [8] S. Zhang, D. A. Genov, Y. Wang, M. Liu, and X. Zhang, Plasmon-Induced Transparency in Metamaterials, *Phys. Rev. Lett.* **101**, 047401 (2008).
- [9] N. Papisimakis, V. A. Fedotov, N. I. Zheludev, and S. L. Prosvirnin, Metamaterial Analog of Electromagnetically Induced Transparency, *Phys. Rev. Lett.* **101**, 253903 (2008).
- [10] P. Tassin, L. Zhang, T. Koschny, E. N. Economou, and C. M. Soukoulis, Low-Loss Metamaterials Based on Classical Electromagnetically Induced Transparency, *Phys. Rev. Lett.* **102**, 053901 (2009).
- [11] N. Liu, L. Langguth, T. Weiss, J. Kästel, M. Fleischhauer, T. Pfau, and H. Giessen, Plasmonic analog of electromagnetically induced transparency at the Drude damping limit, *Nature Mater.* **8**, 758 (2009).
- [12] C. Chen, I. Un, N. Tai, and T. Yen, Asymmetric coupling between subradiant and superradiant plasmonic resonances and its enhanced sensing performance, *Opt. Expr.* **17**, 15372 (2009).
- [13] Z. Dong, H. Liu, J. Cao, T. Li, S. Wang, S. Zhu, and X. Zhang, Enhanced sensing performance by the plasmonic analog of electromagnetically induced transparency in active metamaterials, *Appl. Phys. Lett.* **97**, 114101 (2010).
- [14] N. Liu, M. Hentschel, T. Weiss, A. P. Alivisatos, and H. Giessen, Three-dimensional plasmon rulers, *Science* **332**, 1407 (2011).
- [15] Z. Han and S. I. Bozhevolnyi, Plasmon-induced transparency with detuned ultracompact Fabry-Perot resonators in integrated plasmonic devices, *Opt. Expr.* **19**, 3251 (2011).
- [16] J. Gu, R. Singh, X. Liu, X. Zhang, Y. Ma, S. Zhang, S. A. Maier, Z. Tian, A. K. Azad, H.-T. Chen, A. J. Taylor, J. Han, and W. Zhang, Active control of electromagnetically induced transparency analog in terahertz metamaterials, *Nature Commun.* **3**, 1151 (2012).
- [17] Z. Bai, C. Hang, and G. Huang, Subluminal and superluminal terahertz radiation in metamaterials with electromagnetically induced transparency, *Opt. Expr.* **21**, 17736 (2013).
- [18] T. Nakanishi, T. Otani, Y. Tamayama, and M. Kitano, Storage of electromagnetic waves in a metamaterial that mimics electromagnetically induced absorption in plasmonics, *Phys. Rev. B* **87**, 161110(R) (2013).
- [19] Z. Bai, G. Huang, L. Liu, and S. Zhang, Giant Kerr nonlinearity and low-power gigahertz solitons via plasmon-induced transparency, *Sci. Rep.* **5**, 13780 (2015).
- [20] Y. Sun, Y. Tong, C. Xue, Y. Ding, Y. Li, H. Jiang, and H. Chen, Electromagnetic diode based on nonlinear electromagnetically induced transparency in metamaterials, *Appl. Phys. Lett.* **103**, 091904 (2013).
- [21] T. Matsui, M. Liu, D. A. Powell, I. V. Shadrivov, and Y. S. Kivshar, Electromagnetic tuning of resonant transmission in magnetoelastic metamaterials, *Appl. Phys. Lett.* **104**, 161117 (2014).
- [22] A. C. Newell and J. V. Moloney, *Nonlinear Optics* (Addison-Wesley, Redwood City, 1992), pp. 74–75.
- [23] B. Wang, J. F. Zhou, T. Koschny, and C. M. Soukoulis, Nonlinear properties of split-ring resonators, *Opt. Expr.* **16**, 16058 (2008).
- [24] D. A. Powell, I. V. Shadrivov, and Y. S. Kivshar, Nonlinear electric metamaterials, *Appl. Phys. Lett.* **95**, 084102 (2009).
- [25] E. Poutrina, D. Huang, and D. R. Smith, Analysis of nonlinear electromagnetic metamaterials, *New J. Phys.* **12**, 093010 (2010).
- [26] M. O. Scully and M. S. Zubairy, *Quantum Optics* (Cambridge University Press, Cambridge, 1997).
- [27] A. Jeffery and T. Kawahawa, *Asymptotic Method in Nonlinear Wave Theory* (Pitman, London, 1982).
- [28] M. Ablowitz and P. Clarkson, *Solitons, Nonlinear Evolution Equation and Inverse Scattering* (Cambridge University Press, Cambridge, 1991).